Enhancement of Hippocampal Pyramidal Cell Excitability by the Novel Selective Slow-Afterhyperpolarization Channel Blocker 3-(Triphenylmethylaminomethyl)pyridine (UCL2077)

Mala M. Shah, Mazyar Javadzadeh-Tabatabaie, David C. H. Benton, C. Robin Ganellin, and Dennis G. Haylett

Departments of Pharmacology (M.M.S., D.C.H.B., D.G.H.) and Chemistry (M.J.-T., C.R.G.), University College London, Gower Street, London, United Kingdom

Received May 13, 2006; accepted July 28, 2006

ABSTRACT

The slow afterhyperpolarization (sAHP) in hippocampal neurons has been implicated in learning and memory. However, its precise role in cell excitability and central nervous system function has not been explicitly tested for 2 reasons: 1) there are, at present, no selective inhibitors that effectively reduce the underlying current in vivo or in intact in vitro tissue preparations, and 2) although it is known that a small conductance K^+ channel that activates after a rise in $[Ca^{2+}]_i$ underlies the sAHP, the exact molecular identity remains unknown. We show that 3-(triphenylmethylaminomethyl)pyridine (UCL2077), a novel compound, suppressed the sAHP present in hippocampal neurons in culture ($IC_{50} = 0.5\ \mu M$) and in the slice preparation ($IC_{50} \approx 10\ \mu M$). UCL2077 was selective, having minimal effects on Ca^{2+} channels, action potentials, input resistance and the medium afterhyperpolarization. UCL2077 also had little effect on heterologously expressed small conductance Ca^{2+}-activated K^+ (SK) channels. Moreover, UCL2077 and apamin, a selective SK channel blocker, affected spike firing in hippocampal neurons in different ways. These results provide further evidence that SK channels are unlikely to underlie the sAHP. This study also demonstrates that UCL2077, the most potent, selective sAHP blocker described so far, is a useful pharmacological tool for exploring the role of sAHP channels in the regulation of cell excitability in intact tissue preparations and, potentially, in vivo.

A train of action potentials in hippocampal neurons is followed by an afterhyperpolarization comprising fast, medium (mAHP), and slow (sAHP) components (Storm, 1990; Sah and Faber, 2002). The sAHP has been reported to be important for regulation of spike frequency accommodation and, therefore, neuronal function (Lancaster and Nicoll, 1987; Storm, 1990; Sah and Faber, 2002; Disterhoft et al., 2004). Indeed, these channels have been suggested to have a role in hippocampal memory encoding processes. In particular, enhanced sAHP has been observed in older animals and has been correlated with impairments in learning (Power et al., 2002; Tombaugh et al., 2005). Therefore, sAHP current blockers can potentially be useful for improving learning and

memory. Although it is known that a small conductance K^+ channel that requires Ca^{2+} entry for activation underlies the sAHP (Lancaster and Nicoll, 1987; Sah and Isaacson, 1995; Sah and Faber, 2002), the molecular identity of the channel is still a mystery. Three small conductance Ca^{2+}-activated K^+ channels (SK1–3) have been cloned, of which SK1 and SK2 are strongly expressed in the hippocampus (Stocker et al., 1999). Initial studies suggested that SK1 could be a potential molecular candidate for the sAHP (Kohler et al., 1996; Vergara et al., 1998). However, several more recent studies have indicated that it is unlikely to contribute to the sAHP in hippocampal neurons (Shah and Haylett, 2000b; Strobaek et al., 2000; Grunnet et al., 2001; Shah et al., 2001; Bond et al., 2004; Villalobos et al., 2004). Thus, the progress in our understanding of the contribution of the sAHP channels to cell excitability has been limited by ignorance of the identity of these channels.

In addition, until recently, there were no selective blockers

ABBREVIATIONS: mAHP, medium afterhyperpolarization; sAHP, slow afterhyperpolarization; UCL2027, 2-tritylaminothiazole; FCS, fetal calf serum; HEK, human embryonic kidney; sI_{AHP}, slow afterhyperpolarization current; CGP 55,845, (2S)-3-[[(1S)-1-(3,4-dichlorophenyl)ethyl] amino-2-hydroxypropyl] (phenylmethyl) phosphinic acid; UCL2077, 3-(triphenylmethylaminomethyl)pyridine; HVA, high-voltage-activated; NMDA, N-methyl-D-aspartate.

of the sAHP. The sAHP can be abolished by neurotransmitters such as noradrenaline (Madison and Nicoll, 1982, 1986; Malenka and Nicoll, 1986; Storm, 1990; Sah and Faber, 2002). In the absence of specific inhibitors, these have been used to study the role of the sAHP in cell excitability and behavior. Neurotransmitters, however, have multiple actions, making it difficult to determine whether the effects observed are due to modulation of the sAHP or other currents. For example, noradrenaline blocks the sAHP by elevating cAMP levels and increasing protein kinase A activity (Madison and Nicoll, 1986; Pedarzani and Storm, 1993). cAMP, however, alters the gating of other ion channels, including the hyperpolarization-activated cation channels (Wainger et al., 2001), and can thereby modify cell firing and excitability independently of its effects on the sAHP (Robinson and Siegelbaum, 2003). Although the studies using neurotransmitters to reduce the sAHP have provided significant information regarding the physiological role of the sAHP current, it would be beneficial to revisit the question with more selective blockers to understand the contribution of the current per se to cell excitability.

We have previously described the sAHP inhibitor UCL2027 (Shah et al., 2001). Although this particular blocker suppressed the sAHP in dissociated hippocampal neurons with an IC_{50} of 1 μM, it is very lipophilic and liable to extensive tissue binding. Because the compound also has an aqueous solubility limit of 10 μM, it not ideal for in vitro studies involving slice preparations or in vivo research. In an attempt to find more potent sAHP blockers that might be useful for understanding its physiological role, we synthesized and tested many compounds related to UCL2027 (Zunszain et al., 2002). We now report the actions of a related compound, UCL2077, a more powerful sAHP inhibitor in cultured hippocampal neurons. In addition, it reduced the sAHP in hippocampal neurons present in brain slices. We took advantage of the activity of this compound to explore the role of the sAHP in spike frequency adaptation in hippocampal neurons present in the slice preparation and compared the changes in firing produced by sAHP channel inhibition with that caused by SK channel block.

Materials and Methods

Hippocampal Cell Culture

Hippocampal pyramidal neurons were cultured as described previously (Shah et al., 2001). In brief, 4- to 7-day-old Sprague-Dawley rats were decapitated, and hippocampal regions were subdissected and incubated in Hanks' buffered saline solution containing trypsin. Individual cells were released by trituration and resuspended in Neurobasal medium supplemented with 2% B27, 0.5 mM L-glutamine, and 10% fetal calf serum (FCS). The cells were plated onto plastic dishes (previously coated with poly-D-lysine) and maintained in culture for 15 days using the growth medium without the FCS.

Maintenance and Transfection of HEK293 Cells

HEK293 cells were grown in Dulbecco's modified Eagle's medium supplemented with 2 mM L-glutamine, 50 U/ml penicillin, 50 μg/ml streptomycin, and 10% FCS. Cells were transfected with either hSK1 (kind gift from Dr. J. P. Adelman, Vollum Institute, Oregon Health and Science University, Portland, OR) or rSK2 (kind gift from Dr. W. Joiner and Prof. L. K. Kaczmarek, Department of Cellular and Molecular Physiology, Yale University School of Medicine, New Haven,

CT) and GFP using a modified calcium phosphate method (Shah and Haylett, 2000b).

Hippocampal Slice Preparation

Hippocampal slices were prepared as described previously (Shah et al., 2004). In brief, 5- to 6-week-old Sprague-Dawley rats were anesthetized, brains were removed, and 400-μm slices were cut using a vibratome (Leica, Wetzlar, Germany). The slices were maintained at room temperature in a holding chamber containing external solution (solution A) composed of 125 mM NaCl, 2.5 mM KCl, 1.25 mM NaH_2PO_4, 25 mM $NaHCO_3$, 2 mM $CaCl_2$, 2 mM $MgCl_2$, and 10 mM glucose; pH 7.3 when bubbled continuously with 95% O_2/5% CO_2.

Electrophysiological Studies

Perforated Patch Recordings of sI_{AHP} from Cultured Neurons. The sI_{AHP} was recorded from neurons that had been in culture for at least 8 days as described previously (Shah et al., 2001). In brief, the culture dishes were superfused with solution A also containing 5 mM HEPES and 5 μM DNQX. Perforated patches were obtained at 32–34°C with 4- to 10-MΩ pipettes containing 126 mM $KMeSO_4$, 14 mM KCl, 10 mM HEPES, 3 mM $MgCl_2$, 2 mM Na_2ATP, 0.3 mM Na_2GTP, pH adjusted to 7.3, and 0.12 mg/ml amphotericin. Thirteen action potentials were elicited using 5-ms current pulses (frequency = 76.5 Hz) under discontinuous current-clamp, and the afterhyperpolarization current (sI_{AHP}) produced was recorded under voltage clamp at −55 mV. Voltage and current signals were filtered at 3 and 0.3 kHz, respectively, using an AxoClamp 2A and acquired using pCLAMP 6 software (Molecular Devices, Sunnyvale, CA).

Measurement of Ca^{2+} Currents. Cultured hippocampal neurons possess an extensive dendritic tree and are difficult to voltage-clamp. Ca^{2+} currents were therefore recorded from freshly dissociated cells, which have only a small apical dendrite. Pyramidal cells were isolated and plated as described above and recordings made 3.5 to 8 h after isolation at 32–34°C. The cells were superfused with 115 mM NaCl, 2 mM KCl, 2 mM $CaCl_2$, 0.5 mM $MgCl_2$, 11 mM glucose, 10 mM HEPES, 25 mM TEA, 0.0003 mM tetrodotoxin, and 0.005 mM DNQX, pH adjusted to 7.4. Whole-cell recordings were made with a List EPC-7 amplifier using 7- to 10-MΩ patch pipettes filled with 135 mM CsCl, 0.5 mM $CaCl_2$, 2 mM $MgCl_2$, 10 mM HEPES, 3 mM EGTA, 2 mM Na_2ATP, and 0.3 mM Na_2GTP, pH adjusted to 7.3. The cells were held at −80 mV and the Ca^{2+} current was elicited using a ramp protocol (Fig. 1E). Signals were filtered at 1 kHz and digitized at 3.33 kHz using pCLAMP 6.

Recordings from Hippocampal Cells in Slices. Slices were placed in a recording chamber containing solution A with 0.05 mM DL-2-amino-5-phosphonopentanoic acid, 0.01 mM 6-cyano-2,3-dihydroxy-7-nitroquinoxaline, 0.01 mM bicuculline, and 0.001 mM CGP 55,845 added. The solution in the recording chamber was maintained at a temperature of 33–35°C (Shah et al., 2004). Whole-cell current-clamp recordings were obtained using 10–12 MΩ pipettes filled with 120 mM $KMeSO_4$, 20 mM KCl, 10 mM HEPES, 2 mM $MgCl_2$, 0.2 mM EGTA, 4 mM Na_2ATP, and 0.3 mM Tris-GTP, 14 mM Tris-phosphocreatine, pH adjusted to 7.3. A train of 10 action potentials at a frequency of 66.7 Hz was applied at a holding potential of −60 mV, and the resulting sAHP acquired using an AxoClamp 2B amplifier. Signals were filtered at 30 kHz using the Axoclamp 2B and obtained using pCLAMP 8 software (digitized at 10 kHz).

Measurements of Expressed SK Currents. Cells transfected with either hSK1 or rSK2 subunits 24 h previously and identified by GFP fluorescence, were superfused with 150 mM NaCl, 5 mM KCl, 2 mM $CaCl_2$, 1 mM $MgCl_2$, 10 mM HEPES, and 10 mM glucose, pH adjusted to 7.4 using 1 M NaOH. Whole-cell recordings were made using 3- to 5-MΩ pipettes filled with 130 mM KCl, 5 mM HEDTA, 10 mM HEPES, 3 mM $MgCl_2$, 0.67 mM $CaCl_2$, and 2 mM Na_2ATP, pH adjusted to 7.2 (free $[Ca^{2+}]$ calculated to be 1 μM). Cells were clamped at −80 mV using a List EPC-7 amplifier and voltage pulses

applied to evoke SK currents (Fig. 2A). Signals were filtered at 5 kHz and acquired using pCLAMP 6.

Data Analysis

Data were analyzed using pCLAMP software. The average amplitude of three successive records of sI_{AHP} and sAHP traces in the presence of the drug was expressed as a percentage of that in the absence of the compound. The sI_{AHP} and sAHP decay time constants, as well as the amplitude of the mI_{AHP} recorded in cultured hippocampal neurons, were estimated by fitting a multicomponent exponential equation as described previously (Shah et al., 2001). With the current-clamp experiments done using the slice preparation, the mAHP peak could be easily distinguished by eye in both the absence and the presence of UCL2077 or apamin (Fig. 4).

The input resistance was measured using 1-s hyperpolarizing current pulses of -100 pA from a potential of -70 mV in the absence and presence of the drugs. One-second, depolarizing pulses were applied to study the effects of UCL2077 on the number and frequency of action potentials (see Fig. 5). The minimum current required to evoke a single action potential was used to measure spike threshold. The width and amplitude of the last action potential in the train that was used to evoke the sAHP was also measured in the absence and presence of UCL2077. The action potential width was measured at -20 mV, and the amplitude was measured from the threshold to the tip of the spike.

To investigate effects on the high-voltage-activated (HVA) Ca^{2+} current, the peak average of two successive traces in the presence of the drug were expressed as a percentage of the average peak of the traces acquired immediately before application and after washout of UCL2077. This allowed for alterations in the peak Ca^{2+} current that may occur because of rundown.

SK current steady-state amplitudes in HEK293 cells were measured at -40 mV to minimize the contribution of series resistance errors and the small endogenous delayed rectifier current. The SK current amplitude in the presence of the drug was expressed as a percentage of the average current before addition and after washout of the compound.

All results are expressed as mean $\pm$ S.E. Statistical analysis was carried out using the appropriate Student's t test. Concentration-inhibition curves were fitted with a modified Hill equation (Shah et al., 2001).

Materials

All tissue culture reagents were purchased from Invitrogen (UK). All other materials were acquired from Sigma-Aldrich (UK) apart from apamin and $KMeSO_4$, which were bought from Alamone Labs (Jerusalem, Israel) and Pfaltz and Bauer Ltd. (Waterbury, CT), respectively. UCL2077 (Fig. 1A) was synthesized by authors M.J.-T and C.R.G. Stocks of 100 mM UCL2077 were prepared in dimethyl sulfoxide and kept refrigerated. For experimental purposes, the solutions were diluted at least 10,000-fold in the external solution (final dimethyl sulfoxide concentration <0.01%) because it was found to be insoluble at concentrations >10 μM in our external solution.

Results

Effects of UCL2077 on the sI_{AHP} Recorded in Cultured Hippocampal Neurons. The chemistry program produced a number of compounds related to UCL2027, which were tested for sAHP blocking action using cultured hippocampal neurons (Zunszain et al., 2002). We chose this particular system for two reasons: 1) although it would be more straightforward to test the activity of compounds on expressed channels, the channel underlying the sAHP is unknown, and 2) the sI_{AHP} could be recorded very stably for 1 h, and test compounds could be applied and washed off very
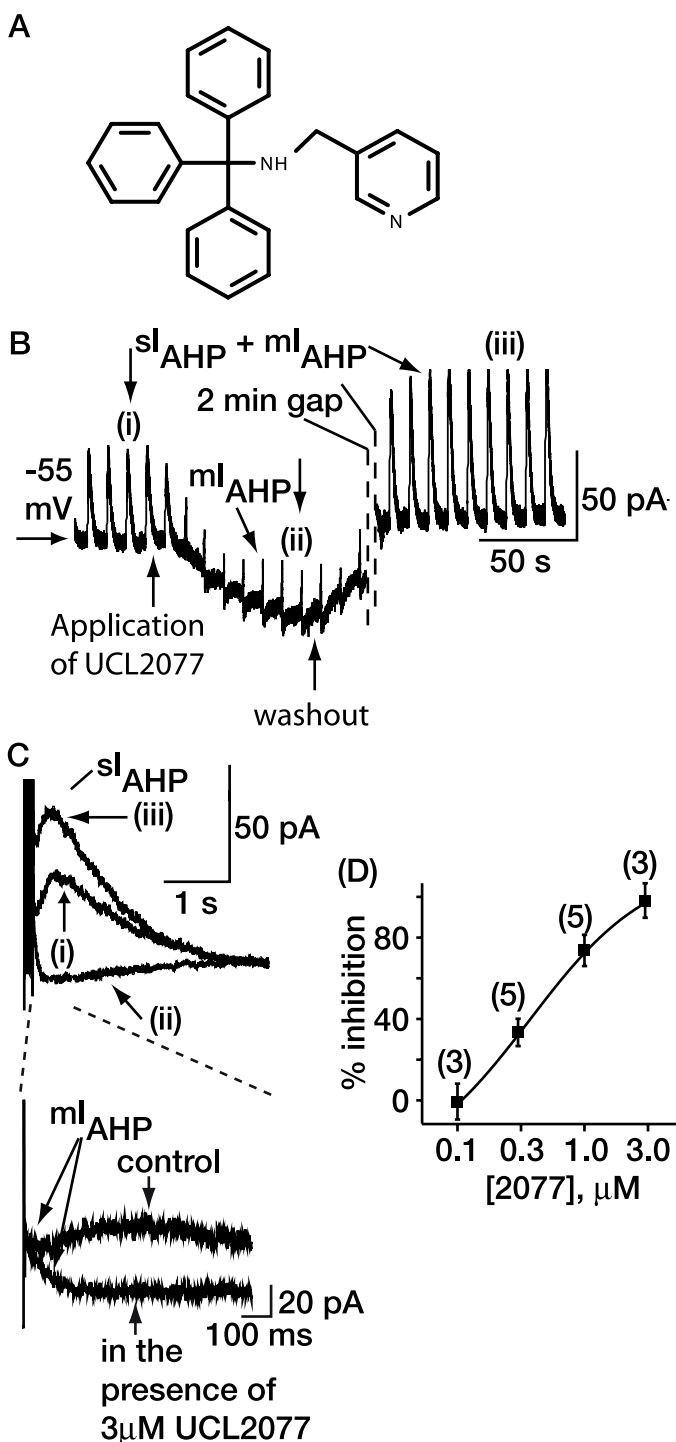

Fig. 1. Effects of UCL2077 on the sAHP recorded from dissociated hippocampal neurons. A, The chemical structure of UCL2077. B, the time course of block of the sI_{AHP} by 3 μM UCL2077 in cultured hippocampal neurons. At -55 mV, there is an outward holding current (in this case, 120 pA), which UCL2077 partially suppressed. The effect on the holding current is variable (between 5 and 40%, as noted in the text). Action potentials have been removed for clarity. The mI_{AHP} was unaffected in the presence of UCL2077, and this is more clearly shown on an enhanced time scale in C. In addition, sometimes the sI_{AHP} increased with time; in this particular cell, that seems to be the case in that there is an over-recovery upon washout of UCL2077. C, effects of UCL2077 shown on an enhanced time scale. The traces shown correspond to (i), (ii), and (iii) in B. D, concentration-inhibition curve for UCL2077. The numbers of observations for each concentration are shown above the symbol.

rapidly (< 1 min). We identified UCL2077 (Fig. 1A) as a potent sI_{AHP} blocker. In contrast to UCL2027, 3 μM UCL2077 abolished the current (Fig. 1, B and C). Maximum effects of the compound were achieved within 2 min and recovery within 5 min (Fig. 1B). The IC_{50} for block of the sI_{AHP} was 0.5 ± 0.1 μM (Fig. 1D), approximately 2-fold more potent than UCL2027 (Shah et al., 2001). Unlike neurotransmitters (e.g., see Malenka and Nicoll, 1986; Krause and Pedarzani, 2000), UCL2077 also had little effect on the decay time constant (τ) or time to peak of the sI_{AHP} (see Table 1).

Furthermore, the mI_{AHP} [due to apamin-sensitive SK channels in cultured hippocampal neurons (Shah et al., 2001)] was unaffected [percentage inhibition = −18.9 ± 10.0% (n = 3)] by 1 μM UCL2077 (Fig. 1). In addition, at concentrations <1 μM, UCL2077 had no effect on resting membrane potential (RMP) under current clamp or the outward holding current under voltage clamp. At 3 μM, UCL2077 reversibly reduced the outward holding current present at −55 mV. The decrease of the outward holding current, however, was very variable, ranging from 5 to 40% (n = 3). Alterations in the
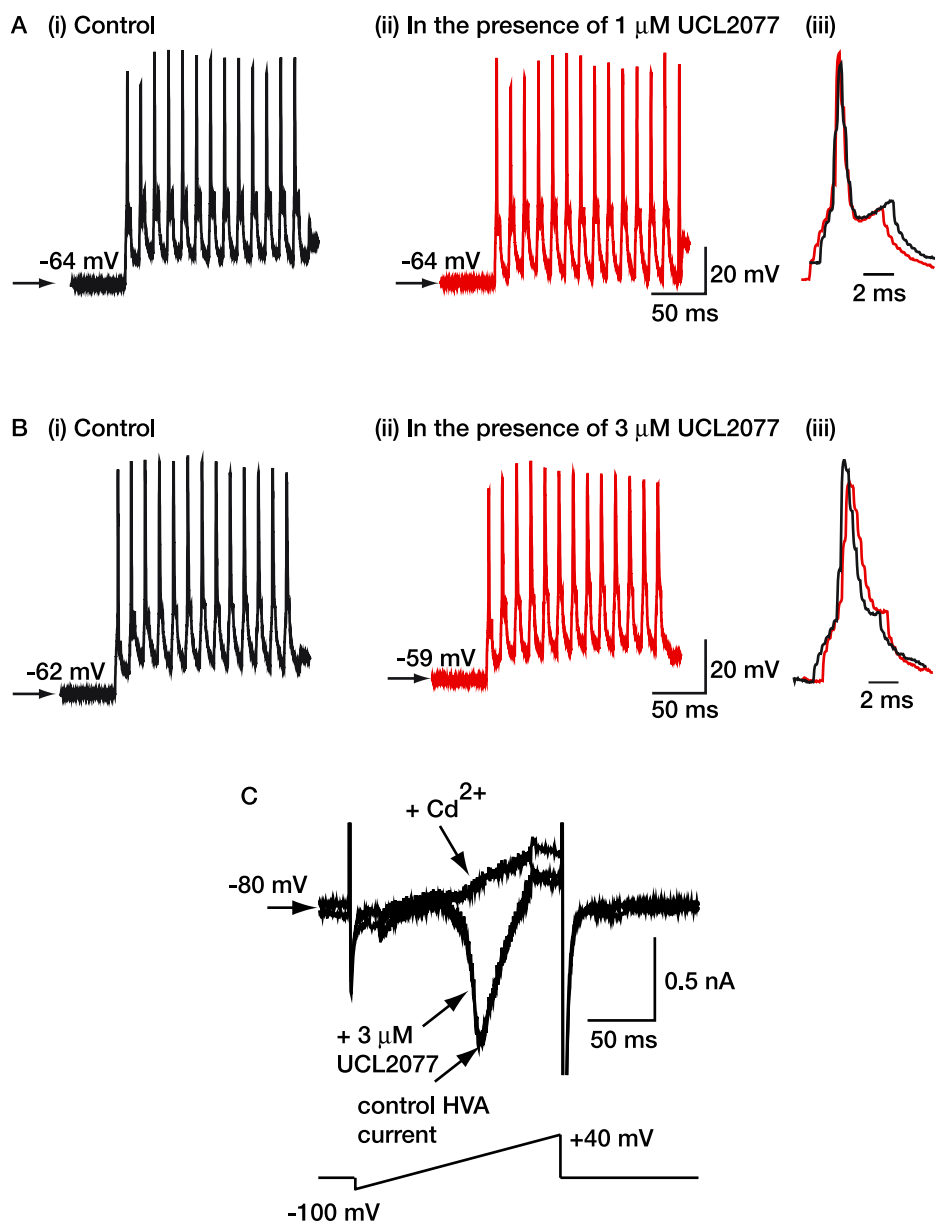

Fig. 2. Effects of UCL2077 on action potentials and the Ca^{2+} current. A and B, trains of action potentials in the absence and presence of UCL2077 when applied at concentrations of 1 and 3 μM, respectively. A (iii) and B (iii) are superimposed records of the last action potential in a train of 13 action potentials before (black) and after (red) application of UCL2077. Note that the resting membrane potential is slightly depolarized in the presence of 3 μM UCL2077, as shown in B (i) and B (ii). The scale bars shown in A (ii) and B (ii) apply to A (i) and B (i), respectively. In addition, the vertical scale bars shown in A (ii) and B (ii) also apply to A (iii) and B (iii), respectively. C, the Ca^{2+} current was elicited by a ramp as shown. Note the traces in the absence and presence of 3 μM UCL2077 overlap. Cd^{2+} (100 μM) was applied to determine the amplitude of the HVA Ca^{2+} current.

TABLE 1
Effects of UCL2077 on action potential shapes and sAHP kinetics in cultured hippocampal pyramidal neurons

	Before Application of UCL2077	In the Presence of UCL2077
Action potential width (1 μM)	1.24 ± 0.2 ms (n = 5)	1.42 ± 0.2 ms (n = 5)
Action potential width (3 μM)	1.90 ± 0.5 ms (n = 3)	2.73 ± 0.6 ms (n = 3)*
Action potential amplitude (3 μM)	68.9 ± 4.0 mV (n = 3)	66.7 ± 1.6 mV (n = 3)
Decay time constant (1 μM)	1.15 ± 0.4 s (n = 5)	0.93 ± 0.4 s (n = 5)
Time to peak (1 μM)	0.50 ± 0.02 s (n = 5)	0.53 ± 0.02 s (n = 5)

* $P < 0.05$.

outward holding current can be equivalent to neuronal depolarization in unclamped cell (Fig. 1B). Indeed, the resting membrane potential depolarized from -62.7 ± 1.2 mV ($n = 3$) under control conditions to -59.3 ± 0.3 mV ($n = 3$, $p = 0.15$) in the presence of 3 μM UCL2077.

It is noteworthy that in two thirds of cells, a slow inward current (an "afterdepolarization") after the action potential train was revealed in the presence of 3 μM UCL2077 (Fig. 1, B and C). A similar current is observed when the sAHP is abolished in CA1 pyramidal neurons (see, for example, Wu et al., 2004). This afterdepolarization may be due to a residual Ca^{2+} current or other channels activated by Ca^{2+} (Caeser et al., 1993; Magee and Carruth, 1999; Wu et al., 2004; Yue and Yaari, 2004).

UCL2077 Effects on Ca^{2+} Influx. Inhibition of the sI_{AHP} might also result from reductions in Ca^{2+} entry caused by either Ca^{2+} channel block or narrowing of action potentials (which are necessary to elicit the sI_{AHP}). We thus measured the effects of UCL2077 directly on the HVA Ca^{2+} current, because Ca^{2+} entry through these channels is likely to be involved in the generation of the sI_{AHP} in hippocampal neurons (Shah and Haylett, 2000a). UCL2077 (3 μM) had no effect on the HVA Ca^{2+} current [inhibition = $1.1 \pm 1.2\%$ ($n = 7$); Fig. 2]. In many cases, it was difficult to distinguish between the low-voltage-activated Ca^{2+} current and the HVA Ca^{2+} current (see Fig. 2C). However, because UCL2077 had little effect on the kinetics of the Ca^{2+} current or the amplitude of the current, it is assumed that it did not affect the low-voltage-activated component either. In addition, at concentrations ≤ 1 μM, it had little effect on action potential width or amplitude (Fig. 2, Table 1). In this respect, UCL2077 is more selective than UCL2027 because UCL2027 causes widening of action potentials at concentrations that block the sAHP by 80% or less (see Shah et al., 2001). Action potential broadening, however, did occur in the presence of 3 μM UCL2077 (Fig. 2, Table 1). Wider action potentials, however, would be expected to increase the Ca^{2+} influx into the cell, leading to sI_{AHP} enhancement, not reduction. These results indicate that UCL2077 does not alter Ca^{2+} influx into neurons.

Effects of UCL2077 on the Cloned SK Channels. Noise analysis studies have indicated that the sAHP channel has a small conductance (2–5 pS; Sah and Isaacson, 1995). Because Ca^{2+} entry is required for the initiation of the sAHP, it has been assumed that a small conductance K^+ channel activated by Ca^{2+} generates the current. SK channels are therefore likely candidates. However, many recent studies, (including ours) have indicated that the SK channels cloned so far are unlikely to underlie the sI_{AHP} (Shah and Haylett, 2000b; Shah et al., 2001; Bond et al., 2004; Villalobos et al., 2004). Nonetheless, we tested the effects of UCL2077 on the cloned SK1 and SK2 channels because these are highly expressed in hippocampal neurons (Stocker et al., 1999). Because rat hippocampal neurons were used, it would be ideal to use the rat homologs of SK channels. However, rSK1 subunits when expressed on their own in heterologous systems do not form functional channels (Bowden et al., 2001; Benton et al., 2003; D'Hoedt et al., 2004). We have thus examined the effects of UCL2077 on channels formed by expression of hSK1 or rSK2 subunits in HEK293 cells. UCL2077 (3 μM) reduced hSK1 and rSK2 current by only $27.2 \pm 3.8\%$ ($n = 4$) and $16.2 \pm 8.9\%$ ($n = 4$), respectively

(Fig. 3). As expected, 10 nM UCL1848, a selective SK channel blocker (Shah and Haylett, 2000b; Hosseini et al., 2001; Benton et al., 2003), reduced the SK1 and SK2 currents by $61.5 \pm 4.3\%$ ($n = 7$) and $90.1 \pm 0.4\%$ ($n = 3$, Fig. 3), respectively. These results show that concentrations of UCL 2077 that affect the sI_{AHP} have much smaller effects on SK channels.

Effects of UCL2077 on sAHP in Hippocampal Neurones in Slices. As noted earlier, it is important to examine

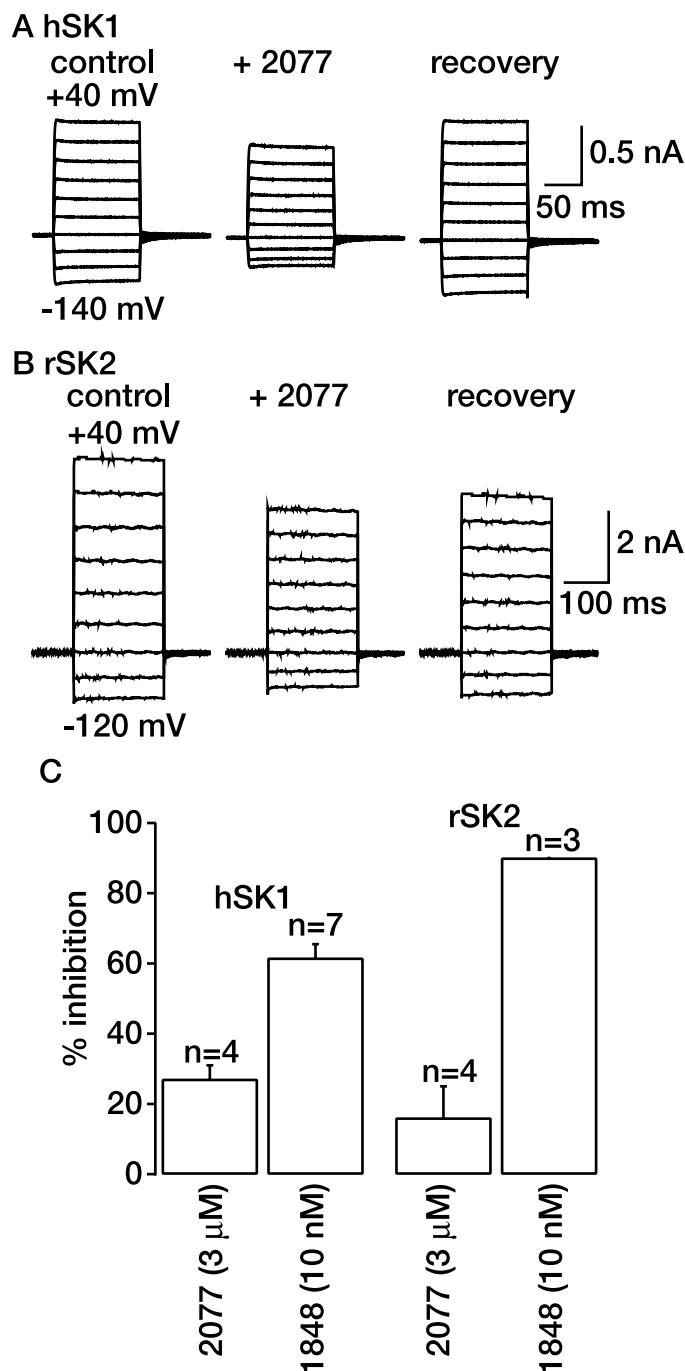**Fig. 3.** Effects of UCL2077 on SK currents. Example traces of hSK1 (A) and rSK2 (B) currents in the absence, presence, and washout of 3 μM UCL2077. The currents were elicited by 100- to 200-ms steps from $-120/-140$ mV to +40 mV from a holding potential of -80 mV. C, summary of effects of 3 μM UCL2077 and 10 nM UCL1848 on SK currents. The numbers of observations for each treatment are shown above the bar.

the activity of this compound on sAHP block in a more intact preparation. Because UCL2077 is 2-fold more potent than UCL2027 (Shah et al., 2001), it seemed worthwhile to test the effects of suppressing the sAHP recorded from visually identified hippocampal neurons present in slices obtained from adult rats. A train of 10 action potentials at -60 mV resulted in a fast afterdepolarization followed by a mAHP

and a sAHP in all cells tested (see Fig. 4). The average sAHP amplitude and decay time constant (τ) were 4.79 ± 0.5 mV ($n = 19$) and 2.05 ± 0.1 s ($n = 19$), respectively. There was also no significant rundown of the AHPs over a period of approximately 1 h (decrease = $0.32 \pm 3.7\%$; $n = 9$). Unlike the cultured neuron system, concentrations of UCL2077 less than 3 μM had little effect on neurons present in the slice

Fig. 4. Effect of UCL2077 on the sAHP in hippocampal neurons present in the slice preparation. A, representative illustrations of the sAHP produced by an action potential train at -60 mV in hippocampal CA1 pyramidal neurons present in the slice preparation before and after application of 10 μM UCL2077. As explained in the text, concentrations of UCL2077 lower than 3 μM were ineffective in the slice preparation; presumably, as is known to occur with many compounds, it is sequestered by tissue. Note that UCL2077 had little effect on the mAHP (shown on an enhanced time scale in the inset). B, time course of the effects of 10 μM UCL2077 on the sAHP shown in A. C, bar graph to show the relative inhibition by 10 μM UCL2077 of the sAHP and mAHP recorded from hippocampal neurons present in the slice preparation. D, records of trains of action potentials in the absence and presence of 10 μM UCL2077. Superimposed traces of the last action potential under control conditions (black) and with UCL2077 present (red) are shown on an enhanced time scale.

TABLE 2
Effects of UCL2077 on action potential and sAHP kinetics measured from hippocampal neurons present in the slice preparation.

	Before Application of UCL2077	In the Presence of UCL2077
Action potential width	1.39 ± 0.5 ms ($n = 8$)	1.31 ± 0.4 ms ($n = 8$)
Action potential threshold	-49.1 ± 2.4 mV ($n = 5$)	-48.2 ± 2.0 mV ($n = 5$)
Action potential amplitude	74.8 ± 2.2 mV ($n = 8$)	69.1 ± 1.9 mV ($n = 8$)
Decay time constant	2.31 ± 0.1 s ($n = 8$)	2.46 ± 0.3 s ($n = 8$)
Time to peak	0.56 ± 0.02 s ($n = 8$)	0.62 ± 0.06 s ($n = 8$)

$* P < 0.05$

preparation. This may be due to tissue sequestration of the compound. In addition, because of limitations in solubility of the compound, concentrations greater than 10 μM cannot be used. We therefore explored the effects of 10 μM UCL2077 on the sAHP. Bath application of this concentration of the compound reduced the sAHP by 60.2 $\pm$ 5.9% ($n = 8$, Fig. 4, A and C), without having a significant effect on the neuronal RMP (the RMP at -60 mV depolarized by 2.3 $\pm$ 1.0 mV ($n = 7$, $p >$ 0.05). The onset of the effects of the compound was slow (approximately 5 min; Fig. 4B) and may be due in part to the slow perfusion rate of 1 ml/min. Maximal block of the sAHP was achieved within 20 min of application and was irreversible up to 20 min after washout in six cells. Partial reversal was obtained in the remaining two neurons. UCL2077 (10 μM) had little effect on action potential width or threshold or the sAHP τ (see Table 2; Fig. 4D). The mAHP was also unaffected (decrease = 7.0 $\pm$ 17%, $n = 6$; Fig. 4, A and C). UCL2077 is thus the first synthetic compound to block the sAHP in more intact tissue preparations and represents a significant step forward in the pharmacology of the sAHP.

Effects of UCL2077 and Apamin on Hippocampal Cell Excitability. As explained in the Introduction, it would be beneficial to evaluate the effects of specifically suppressing the sAHP on cell excitability. Because UCL2077 is the most potent, selective sAHP blocker so far and the only one that is effective in dense tissue preparations such as the slice preparation, we used it to study the effects of a reduced sAHP on spike frequency adaptation using the hippocampal slice preparation. Its actions were compared with those of apamin (an SK channel blocker), because an SK-like channel could underlie the sAHP (Sah and Isaacson, 1995; Vergara et al., 1998).

Application of 10 μM UCL2077 significantly increased the action potential number produced at small current pulses (Fig. 5, A and C) In contrast, treatment with 100 nM apamin [a supramaximal concentration (Stocker et al., 1999)] had no significant effect on action potential number at low current pulses of less than 250 pA in magnitude (Fig. 5C). At higher current pulses ($\geq$250 pA), apamin did substantially increase the number of action potentials, but its effect was significantly less than that of UCL2077 (Fig. 5, B and C). The effects of apamin were irreversible up to 20 min after washout as reported in earlier studies (Stocker et al., 1999). In these same cells, apamin was found to reduce the mAHP evoked by a train of 10 action potentials by 18.5 $\pm$ 0.2% ($n =$ 5). Apamin had no effect on action potential shape (data not shown) or the sAHP (inhibition = $-2.9 \pm 4.5\%$, $n = 5$). Alterations in action potential number could result from changes in a cell's input resistance. Therefore, the input resistance was monitored throughout the recordings and was not significantly altered in the presence of either UCL2077 or apamin (Fig. 5D). These results suggest that sAHP channels are more powerful regulators of spike frequency adaptation than SK channels.

Because the mAHP is short in duration ($<$500 ms), SK channel block may affect the interval between the first few action potentials and thereby modulate the initial firing frequency. We therefore studied the effects of apamin on action potential frequency in the first 250 ms of a 1-s step. Only steps that in the absence of the peptide produced two to four action potentials were used. We found that the spike frequency and thus the interspike interval in the first 250 ms
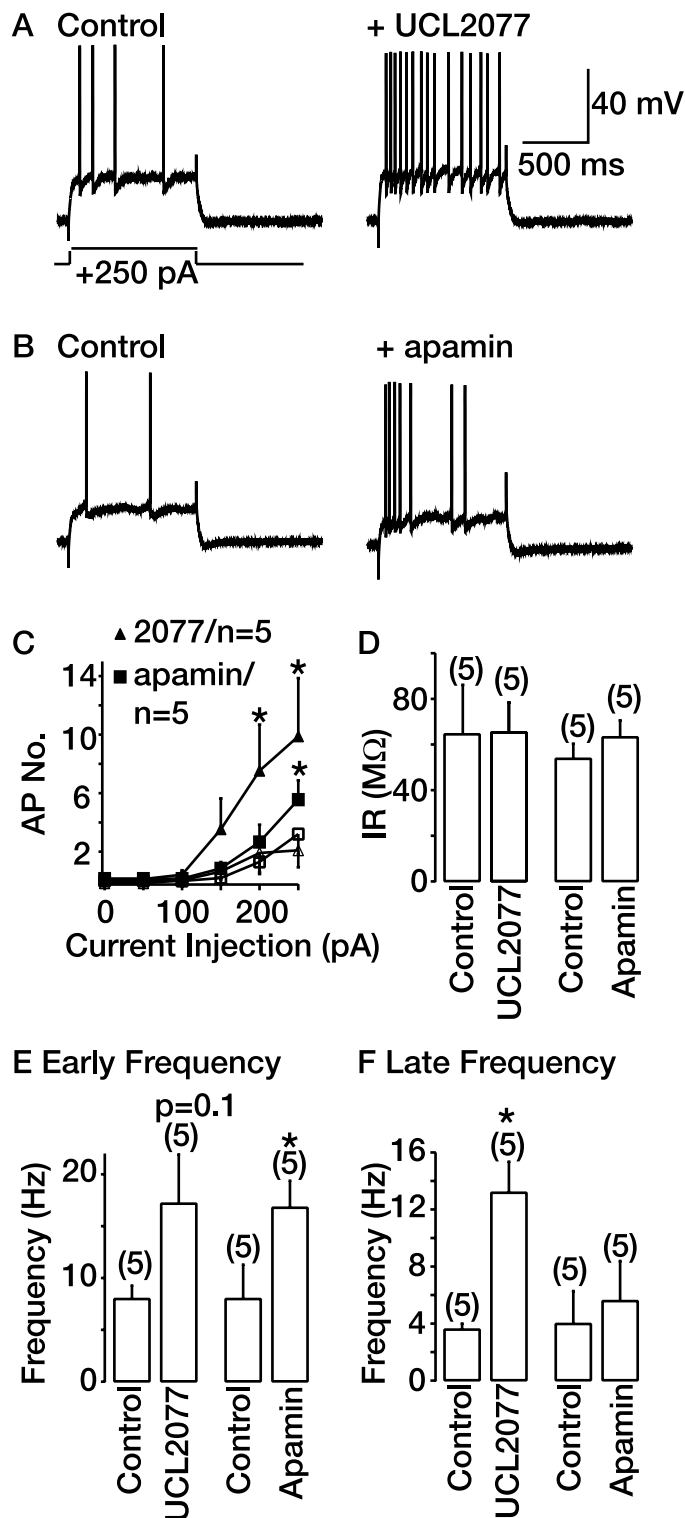

Fig. 5. Comparison of effects of UCL2077 and apamin on spike frequency adaptation in hippocampal neurons. A and B, typical effects of 10 μM UCL2077 and 100 nM apamin on spike-firing when a 250-pA depolarizing pulse is applied from -70 mV. The scale bars shown in A apply to B. C, graph depicting action potential (AP) number produced by current pulses in the absence (open symbols) and presence (closed symbols) of 10 μM UCL2077 or 100 nM apamin. D, E, and F, graphs show the effects of 10 μM UCL2077 and 100 nM apamin on input resistance (IR) and spike frequency within the first 250 ms (E) or the last 250 ms (F) of a 1-s step. $*$, significance at $p < 0.05$.

was indeed altered in the presence of apamin (Fig. 5E). As expected, the firing frequency for the last 250 ms was less affected (Fig. 5F). Thus, SK channels are important for controlling early spike frequency adaptation.

It can be hypothesized that, because of its slow onset and time course, the sAHP would affect firing frequency in the last 250 ms more than in the first 250 ms. Indeed, UCL2077 significantly increased the number of spikes occurring in the last 250 ms (Fig. 5F). It had a nonsignificant but more variable effect during the first 250 ms (Fig. 5E). These results show that the sAHP per se is an influential controller of action potential firing and plays a particularly significant role in affecting spike frequency adaptation.

Discussion

In this study, we report the most potent, direct sAHP blocker produced so far. This particular compound, UCL2077, is also the first of its kind to effectively reduce the sAHP in a slice preparation and thus may be beneficial for in vivo and in vitro studies involving intact tissue preparations. This is a significant step forward in the pharmacology of sAHP suppressors because the only effective blockers described so far are neurotransmitters such as noradrenaline, which are not ideal probes; they affect multiple intracellular processes with effects on multiple channels. Note, however, that 10-fold higher concentrations of UCL2077 were required to block the sAHP in slices than in cultured cells, indicating that the compound might be sequestered by tissue. Hence, even more potent compounds are required for abolition of the sAHP in intact tissue preparations. Nonetheless, we have shown that UCL2077 can be useful for further evaluating the physiological role of the sAHP in in vitro studies and, possibly, by extension in in vivo studies.

UCL2077 had no effect on the Ca^{2+} current or the time course of the sAHP/sI_{AHP} recorded from both cultured hippocampal neurons and hippocampal neurons present in the slice preparation. Partial block of the sAHP by neurotransmitters alters its decay time constant (τ; e.g., see Malenka and Nicoll, 1986; Krause and Pedarzani, 2000). Because τ was unaffected by UCL2077, it indicates that its mechanism of action differs from that of neurotransmitters. It is thus possible that UCL2077 may block the sAHP by directly inhibiting the underlying K^+ channel. Indeed, UCL2077 is a derivative of clotrimazole, which is a known inhibitor of the intermediate conductance Ca^{2+}-activated K^+ (IK) channel (Alvarez et al., 1992; Brugnara et al., 1993; Logsdon et al., 1997; Rittenhouse et al., 1997; Jensen et al., 1998; Hoffman et al., 2003). However, because the molecular identity of the K^+ channel that generates the sAHP is unknown, this hypothesis cannot be directly tested. UCL2077 may, in fact, prove useful in identifying the molecular correlate of the sAHP.

A small conductance K^+ channel activated by Ca^{2+} is believed to underlie the sAHP (Sah and Isaacson, 1995) and thus SK channels can potentially underlie the current (Vergara et al., 1998). We therefore tested the effects of UCL2077 on channels formed by expression of SK1 and SK2 subunits in cultured HEK293 cells. At concentrations that abolished the sI_{AHP} in cultured hippocampal neurons, UCL2077 had little effect on SK current (Fig. 3). Furthermore, SK channels are known to underlie the mAHP in hippocampal neurons

(Stocker et al., 1999; Bond et al., 2004; Villalobos et al., 2004; Gu et al., 2005), and UCL2077 had little effect on the mI_{AHP} in cultured hippocampal neurons (Fig. 1) or the mAHP in hippocampal neurons present in the slice preparation (Fig. 4). Thus, these results provide further evidence that SK channels are unlikely to contribute to the generation of the sAHP in hippocampal neurons, although it cannot be ruled out that the presence of as-yet-unidentified accessory subunits may result in alterations of the pharmacological and biophysical properties of SK channels such that the consequential channel complex generates the sAHP.

We also used the slice preparation and UCL2077 to further evaluate the effects of specifically suppressing the sAHP on hippocampal cell excitability. Consistent with the time course of the sAHP, the number of spikes at the end of a long (>500 ms) depolarizing pulse was substantially increased in the presence of UCL2077 (Fig. 5F). This is in agreement with results from previous studies using neurotransmitters to suppress the sAHP (Storm, 1990; Sah and Faber, 2002). It is noteworthy that there was also a nonsignificant, variable increase in the number of spikes during the beginning of a current pulse in the presence of UCL2077 (Fig. 5E), which might be explained by the suggestion that the sAHP, in addition to the fast afterhyperpolarization and mAHP, can also be activated by a single action potential (Storm, 1990). The effects of UCL2077 were independent of alterations in resting membrane potential, spike threshold (Table 2), input resistance (Fig. 5D), and the mAHP (Fig. 4, A and C), indicating that the compound has little effect on M or h channels, modulation of which can also substantially alter spike frequency adaptation (Aiken et al., 1995; Robinson and Siegelbaum, 2003; Gu et al., 2005). This is an advantage of using UCL2077 over neurotransmitters such as acetylcholine or noradrenaline for studying the physiological role of the sAHP.

Because SK channels have previously been suggested to underlie the sAHP (Vergara et al., 1998), we compared the actions of a specific SK channel blocker with those of UCL2077 on spike frequency adaptation. Unlike UCL2077, the SK channel blocker apamin had a much smaller effect on action potential number (Fig. 5) and only significantly altered early spike frequency adaptation (Fig. 5E). This result indicates that sAHP suppression is likely to generate significantly more somatic action potentials in response to a strong synaptic input and so increase neuronal output. Therefore, more action potentials would back-propagate into dendrites and facilitate opening of NMDA receptor channels by removing the Mg^{2+} block, enhancing further incoming excitatory synaptic inputs and, perhaps, synaptic integration (Johnston et al., 1999). SK channel inhibition may also affect NMDA receptor activation. However, because it is possible that they are located in dendrites and spines near the NMDA receptor, this effect is more likely to be mediated by local dendritic and spine depolarization (Cai et al., 2004; Faber et al., 2005; Ngo-Anh et al., 2005). Thus, SK and sAHP channel blockers affect hippocampal cellular information processing by different mechanisms and may thereby influence learning and memory processes distinctly.

References

Aiken SP, Lampe BJ, Murphy PA, and Brown BS (1995) Reduction of spike frequency adaptation and blockade of M-current in rat CA1 pyramidal neurones by linopirdine (DuP 996), a neurotransmitter release enhancer. *Br J Pharmacol* **115:**1163–1168.

Alvarez J, Montero M, and Garcia-Sancho J (1992) High affinity inhibition of Ca^{2+}-dependent K^+ channels by cytochrome P-450 inhibitors. *J Biol Chem* **267:**11789–11793.

Benton DC, Monaghan AS, Hosseini R, Bahia PK, Haylett DG, and Moss GW (2003) Small conductance Ca^{2+}-activated K^+ channels formed by the expression of rat SK1 and SK2 genes in HEK 293 cells. *J Physiol* **553:**13–19.

Bond CT, Herson PS, Strassmaier T, Hammond R, Stackman R, Maylie J, and Adelman JP (2004) Small conductance Ca^{2+}-activated K^+ channel knock-out mice reveal the identity of calcium-dependent afterhyperpolarization currents. *J Neurosci* **24:**5301–5306.

Bowden SE, Fletcher S, Loane DJ, and Marrion NV (2001) Somatic colocalization of rat SK1 and D class ($Ca_v1.2$) L-type calcium channels in rat CA1 hippocampal pyramidal neurons. *J Neurosci* **21:**RC175.

Brugnara C, de Franceschi L, and Alper SL (1993) Inhibition of Ca^{2+}-dependent K^+ transport and cell dehydration in sickle erythrocytes by clotrimazole and other imidazole derivatives. *J Clin Investig* **92:**520–526.

Caeser M, Brown DA, Gahwiler BH, and Knopfel T (1993) Characterization of a calcium-dependent current generating a slow afterdepolarization of CA3 pyramidal cells in rat hippocampal slice cultures. *Eur J Neurosci* **5:**560–569.

Cai X, Liang CW, Muralidharan S, Kao JP, Tang CM, and Thompson SM (2004) Unique roles of SK and Kv4.2 potassium channels in dendritic integration. *Neuron* **44:**351–364.

D'Hoedt D, Hirzel K, Pedarzani P, and Stocker M (2004) Domain analysis of the calcium-activated potassium channel SK1 from rat brain. Functional expression and toxin sensitivity. *J Biol Chem* **279:**12088–12092.

Disterhoft JF, Wu WW, and Ohno M (2004) Biophysical alterations of hippocampal pyramidal neurons in learning, ageing and Alzheimer's disease. *Ageing Res Rev* **3:**383–406.

Faber ES, Delaney AJ, and Sah P (2005) SK channels regulate excitatory synaptic transmission and plasticity in the lateral amygdala. *Nat Neurosci* **8:**635–641.

Grunnet M, Jensen BS, Olesen SP, and Klaerke DA (2001) Apamin interacts with all subtypes of cloned small-conductance Ca^{2+}-activated K^+ channels. *Pflueg Arch Eur J Physiol* **441:**544–550.

Gu N, Vervaeke K, Hu H, and Storm JF (2005) Kv7/KCNQ/M and HCN/h, but not KCa2/SK channels, contribute to the somatic medium after-hyperpolarization and excitability control in CA1 hippocampal pyramidal cells. *J Physiol* **566:**689–715.

Hoffman JF, Joiner W, Nehrke K, Potapova O, Foye K, and Wickrema A (2003) The hSK4 (KCNN4) isoform is the Ca^{2+}-activated K^+ channel (Gardos channel) in human red blood cells. *Proc Natl Acad Sci USA* **100:**7366–7371.

Hosseini R, Benton DC, Dunn PM, Jenkinson DH, and Moss GW (2001) SK3 is an important component of K^+ channels mediating the afterhyperpolarization in cultured rat SCG neurones. *J Physiol* **535:**323–334.

Jensen BS, Strobaek D, Christophersen P, Jorgensen TD, Hansen C, Silahtaroglu A, Olesen SP, and Ahring PK (1998) Characterization of the cloned human intermediate-conductance Ca^{2+}-activated K^+ channel. *Am J Physiol* **275:**C848–C856.

Johnston D, Hoffman DA, Colbert CM, and Magee JC (1999) Regulation of backpropagating action potentials in hippocampal neurons. *Curr Opin Neurobiol* **9:**288–292.

Kohler M, Hirschberg B, Bond CT, Kinzie JM, Marrion NV, Maylie J, and Adelman JP (1996) Small-conductance, calcium-activated potassium channels from mammalian brain. *Science (Wash DC)* **273:**1709–1714.

Krause M and Pedarzani P (2000) A protein phosphatase is involved in the cholinergic suppression of the Ca^{2+}-activated K^+ current sI_{AHP} in hippocampal pyramidal neurons. *Neuropharmacology* **39:**1274–1283.

Lancaster B and Nicoll RA (1987) Properties of two calcium-activated hyperpolarizations in rat hippocampal neurones. *J Physiol* **389:**187–203.

Logsdon NJ, Kang J, Togo JA, Christian EP, and Aiyar J (1997) A novel gene, hKCa4, encodes the calcium-activated potassium channel in human T lymphocytes. *J Biol Chem* **272:**32723–32726.

Madison DV and Nicoll RA (1982) Noradrenaline blocks accommodation of pyramidal cell discharge in the hippocampus. *Nature (Lond)* **299:**636–638.

Madison DV and Nicoll RA (1986) Cyclic adenosine 3',5'-monophosphate mediates beta-receptor actions of noradrenaline in rat hippocampal pyramidal cells. *J Physiol* **372:**245–259.

Magee JC and Carruth M (1999) Dendritic voltage-gated ion channels regulate the action potential firing mode of hippocampal CA1 pyramidal neurons. *J Neurophysiol* **82:**1895–1901.

Malenka RC and Nicoll RA (1986) Dopamine decreases the calcium-activated afterhyperpolarization in hippocampal CA1 pyramidal cells. *Brain Res* **379:**210–215.

Ngo-Anh TJ, Bloodgood BL, Lin M, Sabatini BL, Maylie J, and Adelman JP (2005) SK channels and NMDA receptors form a Ca^{2+}-mediated feedback loop in dendritic spines. *Nat Neurosci* **8:**642–649.

Pedarzani P and Storm JF (1993) PKA mediates the effects of monoamine transmitters on the K^+ current underlying the slow spike frequency adaptation in hippocampal neurons. *Neuron* **11:**1023–1035.

Power JM, Wu WW, Sametsky E, Oh MM, and Disterhoft JF (2002) Age-related enhancement of the slow outward calcium-activated potassium current in hippocampal CA1 pyramidal neurons in vitro. *J Neurosci* **22:**7234–7243.

Rittenhouse AR, Vandorpe DH, Brugnara C, and Alper SL (1997) The antifungal imidazole clotrimazole and its major in vivo metabolite are potent blockers of the calcium-activated potassium channel in murine erythroleukemia cells. *J Membr Biol* **157:**177–191.

Robinson RB and Siegelbaum SA (2003) Hyperpolarization-activated cation currents: from molecules to physiological function. *Annu Rev Physiol* **65:**453–480.

Sah P and Faber ES (2002) Channels underlying neuronal calcium-activated potassium currents. *Prog Neurobiol* **66:**345–353.

Sah P and Isaacson JS (1995) Channels underlying the slow afterhyperpolarization in hippocampal pyramidal neurons: neurotransmitters modulate the open probability. *Neuron* **15:**435–441.

Shah M and Haylett DG (2000a) Ca^{2+} channels involved in the generation of the slow afterhyperpolarization in cultured rat hippocampal neurons. *J Neurophysiol* **83:**2554–2561.

Shah M and Haylett DG (2000b) The pharmacology of hSK1 Ca^{2+}-activated K^+ channels expressed in mammalian cell lines. *Br J Pharmacol* **129:**627–630.

Shah MM, Anderson AE, Leung V, Lin X, and Johnston D (2004) Seizure-induced plasticity of h channels in entorhinal cortical layer III pyramidal neurons. *Neuron* **44:**495–508.

Shah MM, Miscony Z, Javadzadeh-Tabatabaie M, Ganellin CR, and Haylett DG (2001) Clotrimazole analogues: effective blockers of the slow afterhyperpolarization in cultured rat hippocampal pyramidal neurones. *Br J Pharmacol* **132:**889–898.

Stocker M, Krause M, and Pedarzani P (1999) An apamin-sensitive Ca^{2+}-activated K^+ current in hippocampal pyramidal neurons. *Proc Natl Acad Sci USA* **96:**4662–4667.

Storm JF (1990) Potassium currents in hippocampal pyramidal cells. *Prog Brain Res* **83:**161–187.

Strobaek D, Jorgensen TD, Christophersen P, Ahring PK, and Olesen SP (2000) Pharmacological characterization of small-conductance Ca^{2+}-activated K^+ channels stably expressed in HEK 293 cells. *Br J Pharmacol* **129:**991–999.

Tombaugh GC, Rowe WB, and Rose GM (2005) The slow afterhyperpolarization in hippocampal CA1 neurons covaries with spatial learning ability in aged Fisher 344 rats. *J Neurosci* **25:**2609–2616.

Vergara C, Latorre R, Marrion NV, and Adelman JP (1998) Calcium-activated potassium channels. *Curr Opin Neurobiol* **8:**321–329.

Villalobos C, Shakkottai VG, Chandy KG, Michelhaugh SK, and Andrade R (2004) SKCa channels mediate the medium but not the slow calcium-activated afterhyperpolarization in cortical neurons. *J Neurosci* **24:**3537–3542.

Wainger BJ, DeGennaro M, Santoro B, Siegelbaum SA, and Tibbs GR (2001) Molecular mechanism of cAMP modulation of HCN pacemaker channels. *Nature (Lond)* **411:**805–810.

Wu WW, Chan CS, and Disterhoft JF (2004) Slow afterhyperpolarization governs the development of NMDA receptor-dependent afterdepolarization in CA1 pyramidal neurons during synaptic stimulation. *J Neurophysiol* **92:**2346–2356.

Yue C and Yaari Y (2004) KCNQ/M channels control spike afterdepolarization and burst generation in hippocampal neurons. *J Neurosci* **24:**4614–4624.

Zunszain PA, Shah MM, Miscony Z, Javadzadeh-Tabatabaie M, Haylett DG, and Ganellin CR (2002) Tritylamino aromatic heterocycles and related carbinols as blockers of Ca^{2+}-activated potassium ion channels underlying neuronal hyperpolarization. *Arch Pharm (Weinheim)* **335:**159–166.

Address correspondence to: Mala M. Shah, Department of Pharmacology, University College London, Gower Street, London WC1E 6BT UK. E-mail: mala.shah@ucl.ac.uk